



# 1 Community specific hydraulic conductance potential of soil water 2 decomposed for two Alpine grasslands by small-scale lysimetry

3

4 Georg Frenck<sup>ab</sup>, Georg Leitinger<sup>ab</sup>, Nikolaus Obojes<sup>a</sup>, Magdalena Hofmann<sup>b</sup>, Christian Newesely<sup>b</sup>,  
5 Mario Deutschmann<sup>b</sup>, Ulrike Tappeiner<sup>ab</sup> & Erich Tasser<sup>a\*</sup>

6

7 <sup>a</sup> Institute for Alpine Environment, EURAC research, Viale Druso 1, 39100 Bozen/Bolzano, ITA

8 <sup>b</sup> Institute of Ecology, University of Innsbruck, Sternwartestrasse 15, 6020 Innsbruck, AUT

9

10

11 *Correspondence to:* Erich Tasser ([erich.tasser@eurac.edu](mailto:erich.tasser@eurac.edu))

12

13 **Abstract:** For Central Europe in addition to rising temperatures an increasing variability of precipitation is predicted. This  
14 will increase the probability of drought periods in the Alps, where water supply has been sufficient in most areas so far. For  
15 Alpine grasslands, community specific imprints on drought response are merely understood. In a replicated mesocosm  
16 experiment we compared evapotranspiration and biomass productivity of two differently drought-adapted vegetation  
17 communities during two artificial drought periods divided by extreme precipitation events using high precision small  
18 lysimeters. The drought adapted vegetation type showed a high potential to utilize even scarce water resources combined  
19 with a low potential to translate atmospheric deficits into higher water conductance with biomass production staying below  
20 those measured for the non-drought-adapted type. The non-drought-adapted type, in contrast, showed high water  
21 conductance potential with strongly increasing ET rates when environmental conditions became less constraining. With high  
22 rates even at dry conditions, this community appears not to be optimized to save water and might experience drought effects  
23 earlier and probably stronger. In summary, the vegetation's reaction two co-varying gradients of potential evapotranspiration  
24 and soil water content revealed a clear difference of vegetation development and between water-saving and water-spending  
25 strategies regarding evapotranspiration.



26        Comprehensive alterations in the climate system of the earth are projected for the future decades. Due to increased  
27        greenhouse gas concentrations in the atmosphere, the global average temperature is predicted to rise. These changes in the  
28        energy budget of the atmosphere are suggested to propagate alterations in atmospheric circulation and modify precipitation  
29        patterns worldwide (IPCC, 2013; Knapp et al., 2008; Solomon et al., 2009). Such variations can result in changes of the  
30        spatial distribution of precipitation and thereby affect average values of rainfall locally. However, concurrent changes in the  
31        temporal occurrence are predicted to increase the variability of rainfall with longer intervals in between and more extreme  
32        events. This will lead to stronger variability in soil water availability and longer droughts (IPCC, 2013, 2012).

33        The water balance in terrestrial ecosystems is dominantly controlled by plant processes. It is suggested that up to 80%  
34        of the terrestrial water loss to the atmosphere is mediated through plant transpiration (Jasechko et al., 2013). Consequently, it is  
35        assumed that plants will experience drought stress more frequently, which may constrain primary productivity as the latter  
36        is substantially controlled by the supply of water (Knapp et al., 2008). These direct effects of limited water provision to the  
37        system will be accompanied by increased water demand in a warmer world, leading to more negative water balances, which  
38        will accentuate drought effects on vegetation processes (Heimann and Reichstein, 2008). However, structure and  
39        functionality of the ecosystems - defining rates of evapotranspiration - are also subject to local climatic conditions. Hence, a  
40        direct feedback mechanism is established, which might amplify or dampen the global and local consequences of climatic  
41        change on ecosystems (Heimann and Reichstein, 2008).

42        Defining productivity-precipitation relationships of ecosystems is of focused interest, because structural changes in  
43        soil-plant-atmosphere interface, which control water fluxes into the atmosphere will inherently be affected by the  
44        manifestation of that relationship. However, beyond the direct implications of limited water availability on biomass  
45        production and growth, the composition of individual plant species in the community and resulting functional structure of  
46        that community will adjust, optimising water use according to different life-history strategies by competitive interactions  
47        (Peñuelas et al., 2004). In turn, immediate vegetation responses to fluctuations in precipitation patterns and the strength of  
48        interaction with productivity functions will strongly depend on the functional composition of the community and ecosystem  
49        considered. Therefore, intrinsic characteristics of vegetation will impose another layer of complexity for defining the  
50        interactive feedbacks in the relationship between water budget and productivity.

51        The impact of shifting precipitation regimes can be predicted only inaccurately if the crucial components of the  
52        ecosystem water budget - soils, plants and the atmosphere - are evaluated separately and isolated. Due to the complex  
53        interactions and processes at different spatio-temporal scales the response of ecosystems to shifts in the water regime are  
54        preferably examined in an integrative manner on the system level (Silva, 2015). Manipulative experiments are a well suited  
55        option for investigating the effects imposed by changes in precipitation frequency and intensity below and above the natural  
56        range on the ecosystem level (Estiarte et al., 2016). Since we currently lack knowledge needed to validate the projections for  
57        consequences of future changes in rainfall regimes, insights from such integrative investigations are highly valuable for  
58        providing important benchmarks of model based assessments (Estiarte et al., 2016).



59 Numerous studies were performed to reveal the response of temperate grasslands to climatic changes and extremes,  
60 while only few investigations targeted Alpine systems (De Boeck et al., 2016). While the Alps did not often experience  
61 droughts during the past (van der Schrier et al., 2007), the region has undergone exceptionally fast climatic changes during  
62 the late 19<sup>th</sup> through early 21<sup>st</sup> century (Auer et al., 2007; Beniston, 2005; Böhm et al., 2001; Ciccarelli et al., 2008; Rebetez  
63 and Reinhard, 2008). Considering the fundamental role Alpine systems have to water accumulation and freshwater supply  
64 for large parts of Europe (Messerli et al., 2004; Viviroli et al., 2003) it seems surprising that the responses of ecosystems in  
65 the Alps to changes in precipitation have not drawn more scientific attention. However, while projections suggest only  
66 moderate variations of yearly average rainfall in the Alps, significant alterations within the temporal occurrence of rainfall  
67 events with a decrease in summer precipitation and increases from winter through spring are implied (Beniston, 2012;  
68 Beniston et al., 2007). The decrease of water supply during warmer summer months will potentially increase the frequency  
69 and intensity of drought events in the near and longer future in Alpine ecosystems (Gobiet et al., 2014).

70 For unravelling ecosystem water fluxes at the soil-plant-atmosphere interface, the lysimeter methodology provides the  
71 precise and realistic means by allowing to decompose the driving sub-processes: evapotranspiration (ET), precipitation (P)  
72 and drainage below the rooting zone (Peters et al., 2014). By avoiding systematic errors prone to traditional measurement  
73 systems, the determination of the net water balance is highly accurate and robust (Schrader et al., 2013). If embedded into a  
74 surrounding ecosystem, automated lysimeter units, which do not need access to perform manual weighing, measure water  
75 fluxes with a minimum of disturbance to the natural boundary layer and microclimatic conditions. Such implementations of  
76 autonomous weighable high precision lysimeters provide unprecedented realism to the description of ecosystem water  
77 balances, especially when filling of the lysimeters was performed to maintain natural soil layering and the connectivity of  
78 pores, while keeping potential impacts on the vegetation community low. Over the recent years, several of these units have  
79 been established over Europe, e.g. a network of 126 lysimeters at 12 sites has been established to monitor climate chance  
80 induced alterations in hydrological cycling within the TERENO project in Germany (Bogena et al., 2006; Zacharias et al.,  
81 2011). However, the large dimensions (1m diameter/ volume) and the corresponding economic efforts for their establishment  
82 did mostly eliminate the possibility for replicated manipulative experiments employing fully integrated lysimeters.

83 In a common garden experiment we used a network of automated small scale lysimeters to emerge community  
84 specific differences in the temporal dynamics of soil water depletion and evapotranspiration. Two different Alpine grassland  
85 communities were subjected to contrasting levels of water availability. Sheltered from natural precipitation, soil water  
86 content was manipulated by applying two distinct irrigation regimes: one providing water in regular intervals and another  
87 exposing the corresponding experimental units to extended periods of drought. The natural variability in the atmospheric  
88 demand of water vapour coupled to the manipulated water availability in the soil allowed to investigate and reveal vegetation  
89 specific conductance properties and water utilisation patterns. For this study we hypothesize that the vegetation adapted to  
90 local, humid conditions and characterized by high biomass and a water spending strategy will keep transpiration rates high  
91 while soil water availability is decreasing until a sudden decline near wilting point. As a consequence it will also continue to



92 produce biomass until the break point. In contrary, the water saving strategy of the drought-adapted vegetation will lead to a  
93 continuous decrease of transpiration and biomass production with decreasing soil water availability.

## 94 **2.1 Characteristics of the experimental field site and lysimeter installation**

95 The study site of the experiment was established during early summer 2014 in the LTER-Austria site ‘Stubai’ (valley  
96 bottom meadow) Neustift im Stubaital . The site for the garden-experiment was located on the valley floor at 972 m a.s.l.  
97 (WGS84: N47.115833, E11.320556) in a meadow used for hay production.

98 **Table 1 Summary of site conditions and vegetation properties**

site	Stubai (S) – study site location	Matsch/Mazia (M) – transplant origin
municipality	Neustift im Stubaital, Wipptal/Austria	Mals/Malles, Vinschgau/Italy
elevation/ altitude (m a.s.l.)	970	1570
longitude/ latitude	47°07'05“N 11°19'17“E	46°41'19“N 10°34'42“E
average temperature (°C)	6.5	6.6
average precipitation (mm)	1097.0	526.7
growing season length (no of days with average temperature of at least 5 °C)	224	190
land-use	hay meadow/ 3cuts per yr/ fertilized with cow dung	hay meadow/ 2cuts per yr/ fertilized with cow dung 
soil type	gleyed Camisol (A-Bv-Go)	Camisol (Ah-Bv-C) 
classification	loamy sand to sandy silt	loam to sandy loam
phytosociological classification	Poo trivialis - Alopecuretum pratensis (Regel 1925)	Ranunculo bulbosi-Arrhenatherum (Ellmauer)
species inventory (responsible for 90% of total plant cover in the lysimeter)	<i>Achillea millefolium</i> , <i>Carum carvi</i> , <i>Pimpinella major</i> , <i>Poa trivialis</i> , <i>Ranunculus acris</i> , <i>Rumex acetosa</i> , <i>Taraxacum officinale</i> , <i>Trifolium pratense</i>	<i>Achillea millefolium</i> , <i>Anthoxanthum odoratum</i> , <i>Anthriscus sylvestris</i> , <i>Carum carvi</i> , <i>Festuca rubra</i> , <i>Leontodon hispidus</i> , <i>Lotus corniculatus</i> , <i>Poa trivialis</i> , <i>Primula veris</i> , <i>Taraxacum officinale</i> , <i>Trifolium montanum</i> , <i>Trifolium pratense</i> , <i>Veronica officinalis</i>

99  
100 For this experiment six plots of 3.5 × 3.5 m were established. Traversing the corresponding area, each plot was  
101 defined by installing half-cylindrical metal frames. In the centre of each plot these frames providing the base for the rain  
102 sheltering reached a height of approx. 2.5 m. In each corner at the outer plot margin four irrigation sprinklers pointing



103 towards the centre of the plot were set up. The irrigation system described in detail by (Newesely et al., 2015) was used to  
104 simulate precipitation during periods of experimental manipulation of water provision to the system.

105 In the centre of each plot two small-scale lysimeters with 0.3 m diameter were installed in collaboration with, and  
106 supervised by the employees of the manufacturer (Smart-Field-Lysimeter, UMS/Meter Group Munich, Germany). Every  
107 lysimeter was filled with a soil-vegetation monolith by cutting the hollow cylindrical lysimeter blank into an undisturbed  
108 patch of the corresponding ecosystem. This compression free procedure allowed to remain the original and unaffected  
109 stratification of the soil and to conserve the natural composition of pore spaces within the monolith. The filled lysimeter  
110 blanks were subsequently excavated and cut horizontally at a depth of 0.3m. The bottom of the lysimeter was closed with a  
111 tension controlled hydraulic boundary connected to a bi-directional pumping system to regulate water flow into and out of  
112 the lysimeter. After inserting soil moisture, temperature (EC-5 Small Soil Moisture Sensor, Decagon Devices, USA) and  
113 matrix potential probes (MPS-2, Decagon Devices, USA) at 0.05, 0.15 and 0.25m depth into the lysimeter monolith, each  
114 system was placed on a weighing platform (accuracy of 0.005 kg, PL-50, UMS/Meter Group Munich, Germany). Two of  
115 these lysimeter units were installed in the centre of every experimental plot within a two by two quadratic grid of 1.2m edge  
116 length with their relative position to each other assigned randomly.

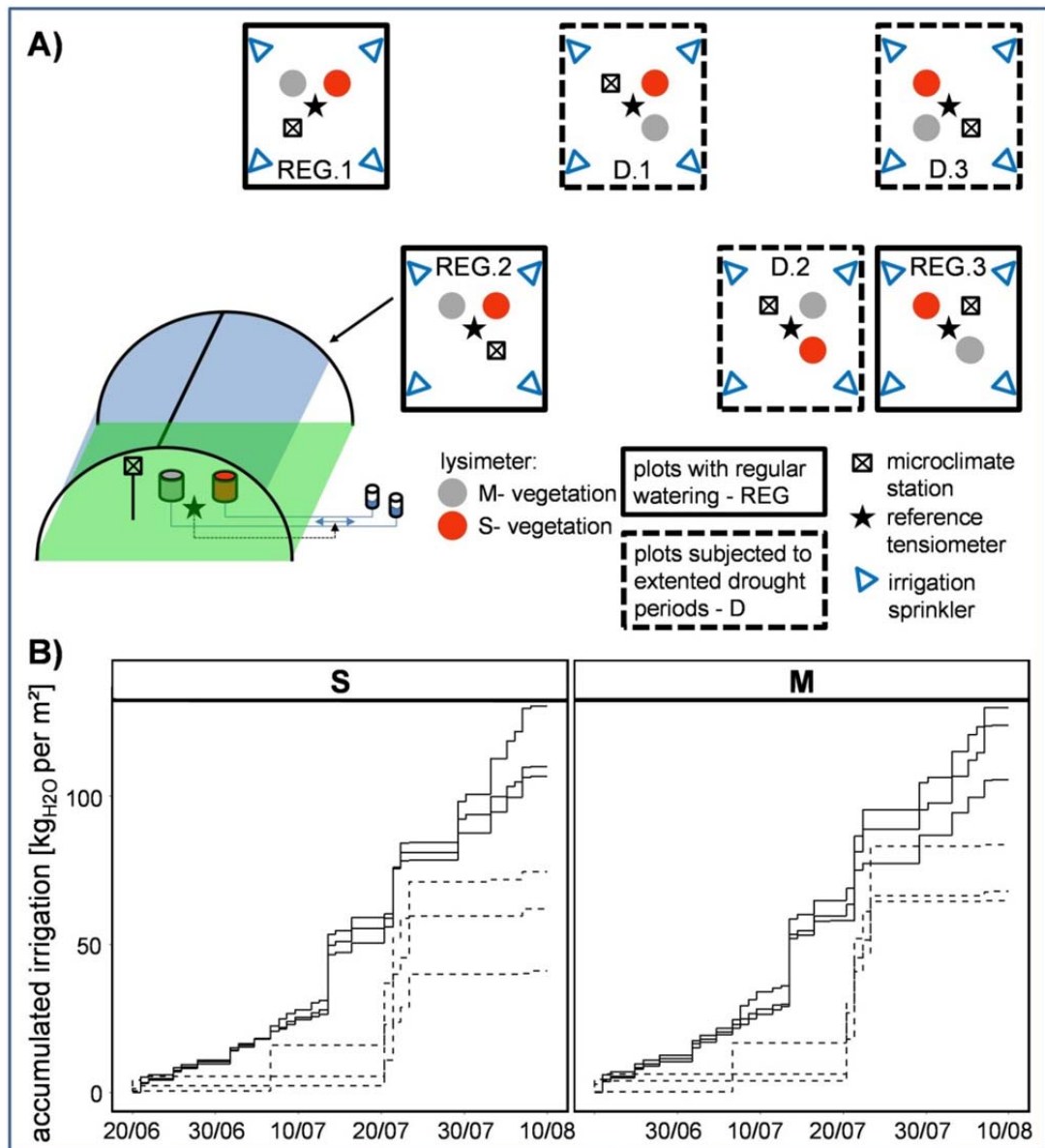
117 The two monoliths in every plot were excavated from different types of vegetation, one containing a mesocosm of the  
118 meadow surrounding the experimental field site (S, Table 1), and another one which was excavated and transplanted from  
119 Matsch/Mazia with contrasting environmental and biotic properties to those of the study site (M, Table 1). The Stubai  
120 grassland is classified as *Poo trivialis - Alopecuretum pratensis* with a community of low complexity: abundant Poaceae  
121 accompanied by some herb species (Wohlfahrt et al., 2008). The meadow is actively managed, cut two to three times each  
122 year and fertilized with cow manure in spring and autumn (approximately 0.35 kg dry matter per m<sup>2</sup>, Table 1). The local  
123 climate is dominated by high total precipitation values, especially in the summer. The vegetation of second origin  
124 (Matsch/Mazia) is characterised by the traditional, more extensive use of the corresponding system. The Matsch Valley has a  
125 dry inneralpine climate with a mean precipitation of 527 mm per year and a mean temperature of 6.6 °C (Hydrographical  
126 Department of the Autonomous Province of Bozen-South Tyrol). The vegetation is a dry hay meadow (*Ranunculo bulbosi -*  
127 *Arrhenatherum*, Ellmauer) on loam to sandy loam. The site is fertilized with cow dung and cut two times each year. The  
128 excavation location of the replicate lysimeters was optimized according to the presence of representative and joint species in  
129 the respective vegetation patches. After installing the local and transplanted lysimeter mesocosms during early summer 2014  
130 into the experimental plots, the vegetation surrounding the lysimeters could recover from disturbances of necessary soil  
131 works required to wire the fully automated measuring system until spring 2015.

132 At the field site, all experimental plots and the vegetation in the lysimeters was managed (cut, fertilized) concurrently  
133 to land-use scheme of the surrounding meadow. The experimental period started in the last third of June 2015 during the re-  
134 growth interval after the first cut at the beginning of June. With beginning of the experiment rain shelters were closed using a  
135 UV permeable transparent polythene film (Lumisol Clear AF, 88% - 92% light transmittance). In order to avoid shielding of



136 the wind and to allow the establishment of natural boundary conditions, shelters were left open on the sides facing the main  
137 wind direction and closed down to just 0.5 m above the soil level on the lateral sides. Over a period of 52 days the plots of  
138 the experiment were subjected to control watering within the two different irrigation schemes (Fig. 1). Concurrently with  
139 closing of the rain shelters precipitation was provided from the irrigation sprinklers mimicking average rain fall amounts and  
140 intensities for the 30 year period between 1970 through 2000 in the treatment with regular watering. However, due to a  
141 mistake by the technician responsible for setting up the automated irrigation protocol the watering scheme stayed below the  
142 intended amounts for approximately the first half of the experimental period making manual compensation occasionally  
143 necessary. Automated irrigation was programmed to occur around mid-night in order to avoid immediate transpiration from  
144 the surface and allow the provided water to penetrate into the soil compartment. Manual adjustments and checks on the  
145 precipitation simulator were usually performed during day-time. The lysimeter mesocosms in the treatments with regular  
146 watering (REG) received approx. 117 kgH<sub>2</sub>O per m<sup>2</sup>, those in the treatments with extended drought periods an average of 65  
147 kgH<sub>2</sub>O per m<sup>2</sup> throughout the duration of the experiment and according to the scheme presented in Fig. 1.







153 **2.2 Automated measurements**

154 In the centre of each of the six plots a microclimate station measuring air temperature and relative humidity (height:  
155 1m; U23-002 HOBO® External Temperature/Relative Humidity Data Logger, Onset Computer Corporation, USA), solar  
156 radiation (height: 1m; S-LIB-M003, Solar Radiation Sensor, Onset Computer Corporation, USA), wind speed (height: 1 m;  
157 DAVIS® Standard Anemometer 7911, Davis Instruments, USA) and soil water content 0.05 and 0.2m below the ground (S-  
158 SMA-M005, Soil Moisture Smart Sensor – 0.2 m ECH2O® probes, Decagon, USA) was installed. The corresponding  
159 measurements were logged for every ten minutes interval (HOBO Microstation® Data Logger; Onset Computer Corporation,  
160 USA).

161 For each of the lysimeter, weight data were recorded every minute, data received from matric potential, soil  
162 temperature and water content sensors (each in 0.05, 0.15 and 0.25 m depth) in ten minutes intervals. The hydraulic  
163 boundary at the bottom of each lysimeter was connected to a reservoir of drainage water with the corresponding container  
164 also being placed on a balance. A bi-directional pumping system allowed the adjustment of the water content at the lower  
165 boundary of the lysimeter by transferring water either from the drainage container into the lysimeter or the contrary  
166 direction. This implementation allowed to adjust the water levels at bottom of the lysimeter according to a reference matric  
167 potential measured at the same depth in the natural unaffected soil column of the respective experimental plots.  
168

169 **2.3 Manual measurements of biomass development**

170 Since variation in total water flux from vegetation canopies to the atmosphere is a product of the variation in standing  
171 biomass and the water vapour release per unit biomass decomposing and addressing these two factors is advisable, especially  
172 in replicated experiments or when communities with different biomass progression rates are being compared over longer  
173 periods. However, non-destructive biomass estimation of complex stands in the field can be challenging with respect to  
174 desired accuracy. In order to generate robust estimates different methodologies were combined in current experiment.  
175 Measurements of maximum and average canopy height (Machado et al., 2002) were supplemented with a pin point  
176 procedure (Jonasson, 1988) and measurements of projected area (Lati et al., 2013) for the estimation of biomass present in  
177 the lysimeters. For measuring pin contacts a thin metal rod was lowered through a plate placed above down to the lysimeter.  
178 Pin measurements were replicated in seven (out of 21) randomly assigned positions for each lysimeter and point in time. Pin  
179 contacts were referenced within three height classes (0-20, 20-40, 40+ cm above the ground) and by functional group  
180 identity of the plants. For the determination of projected area of the lysimeter canopies the methodology proposed by  
181 Tackenberg (2007) was adapted. Digital images of the lysimeter stands in front of a white half-cylindrical background were  
182 scaled according to a size standard in each picture, converted to a black-white colour scheme, before black pixels were  
183 enumerated. On average, biomass of the lysimeters was estimated for every third day through the period of the experiment.  
184 The different methods for non-destructive biomass estimation were calibrated against weighted biomass at the harvests prior



185 and subsequent to the experiment. Based on these calibrations the biomass development in the lysimeters was predicted  
186 throughout the experimental period.

187

188 **2.4 Data processing and statistics**

189 To calculate the water mass fluxes at the soil-vegetation-atmosphere interface of the upper lysimeter boundary,  
190 weight differentials of the drainage reservoir and the lysimeters were summarized and subsequently cleared for spikes and  
191 signals of implausible strength (Schrader et al., 2013). The latter was necessary because the sensitive weighing elements are  
192 susceptible to environmental noise or accidental interference by other experimental proceedings (e.g. biomass estimation),  
193 while providing a high accuracy and temporal resolution. The combined weight signal was separated into irrigation induced  
194 weight gain of the lysimeter units and weight loss caused by evapotranspiration from the upper lysimeter boundary based on  
195 the recorded activity times of the precipitation simulator. Subsequently, daily totals were calculated for both mass  
196 differentials.

197 A soil-specific calibration of the soil moisture and the MPS-2 sensors ~~sensor~~ is a necessary prerequisite ~~for a sensor~~ to  
198 achieve its highest degree of absolute accuracy in soil water content (SWC) measurements. A substrate moisture retention  
199 curve (pF vs. volumetric water content) and the hydraulic conductivity as a function of pF (log10 of the matric potential)  
200 were determined for both types of soil-vegetation monoliths (M, S). The soil hydraulic parameters were determined in the  
201 laboratory, using the method of (Schindler, 1980) with the HYPROP system (UMS/Meter Group Munich, Germany). Using  
202 the soil specific moisture retention curve, absolute SWC was corrected based on soil matrix potential data. To summarize the  
203 time course of water availability in the soil of each lysimeter unit, the average values of SWC of both layers between 0.05 -  
204 0.15m and 0.15 – 0.25m were integrated and summarized on a daily basis.

205 The evaporative demand of the atmosphere is expressed by the reference crop evapotranspiration ( $ET_0$ ). It represents  
206 the evapotranspiration from a standardized vegetated surface and was calculated in this study after the FAO Penman-  
207 Monteith standard method (Allen et al., 1998).  $ET_0$  integrates the most important atmospheric components (solar radiation,  
208 temperature, VPD and wind velocity) defining the atmospheric water demand. Daily averages were used as a summed up  
209 explanatory parameter to capture the atmospheric draw of water vapour from the lysimeter vegetation for further analysis.

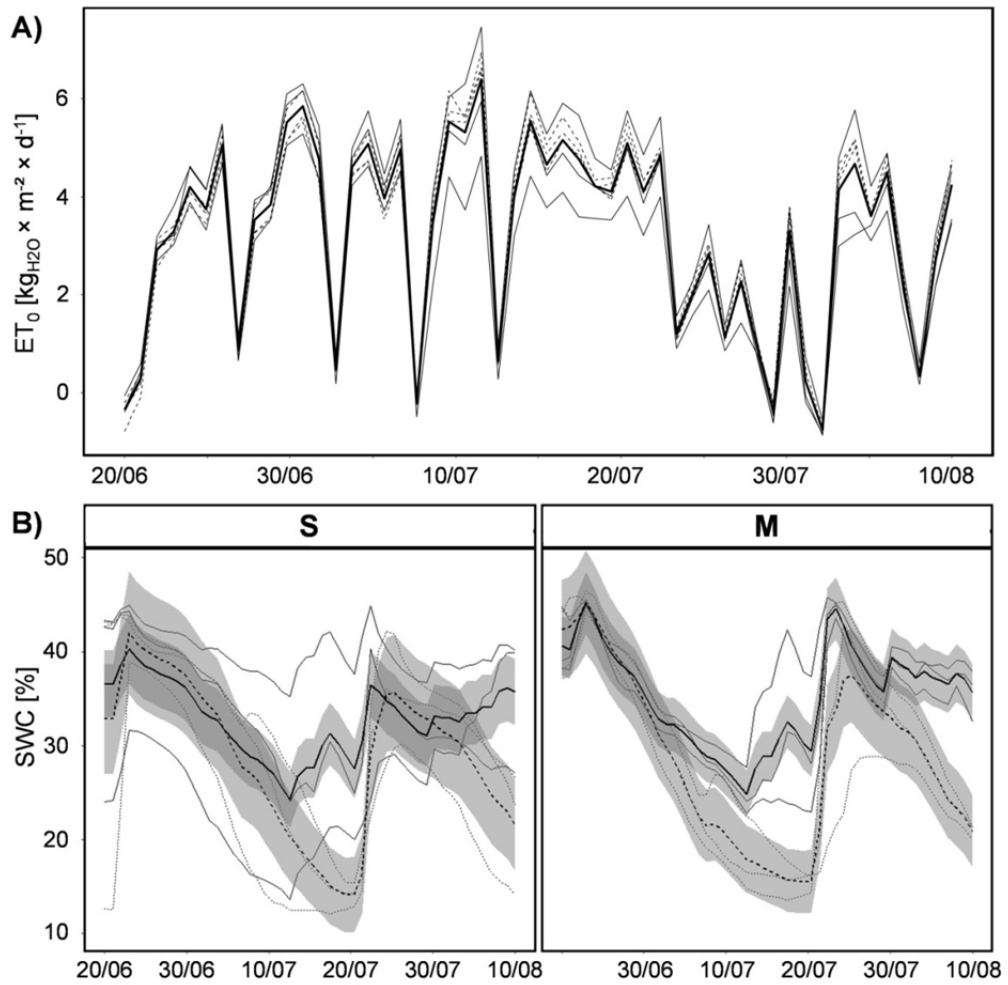
210 Non-destructive estimates for the standing biomass in the lysimeters were calibrated at the harvests before and after  
211 the experimental period. Nine different regression models were generated for the different estimation techniques individually  
212 and in combinations (appendix 1). Based on the prediction of these models biomass was estimated for every measurement  
213 (total of 16) during the experiment. Generating a consensus time-course for the biomass development in every lysimeter a  
214 general additive mixed model smoother was fitted for each unit (gamm-function in the mgcv-package, R Development Core  
215 Team, 2015) with the different prediction methodologies defining random (observer) - effects. In order to generate a more  
216 conservative pattern, the flexibility of the time course defined with these smoothers was constrained by allowing a maximum



217 of five knots for these smoothers. Based on these models, standing biomass was predicted on a dry weight basis for ~~every~~  
218 lysimeter ~~entity~~ and ~~each~~ day of the experiment.

219 All statistical analysis presented here were performed using the R statistical programming language (R Development  
220 Core Team, 2015). For the evaluation of evapotranspiration ~~responses~~ mixed effects models were fitted using the *nlme*-  
221 package. These models included the identity of the different vegetation types (categorical) in full factorial combination with  
222 ~~additional covariates~~ defining the fixed part of the model. To reveal the drivers of variation in daily ET rates and separate the  
223 effects of variability in biomass (DW –dry weight) and evapotranspiration rates per unit biomass (ET/DW) among the  
224 different monoliths a log-log-scaling method was applied on the formula  $ET = ET/DW \times DW$  based on the methodology  
225 provided by (Renton and Poorter, 2011). For summarizing the time courses of SWC and  $ET_0$  the day of the experiment and  
226 the two irrigation schemes were considered as additional categorical variates. For modelling the response surface of ET  
227 along the two dimensions of  $ET_0$  and SWC, ~~the latter and all possible interactions with vegetation type were defined as~~  
228 ~~continuous covariates for the fixed part of the model~~. However, all models included a random intercept for the experimental  
229 plot in which the data were collected. Nested within the random effect for the plot, the lysimeter identity was included as  
230 another random effect to fully represent the dependence structure in the hierarchical design of the experiment. ~~Were~~ they  
231 were found to significantly improve the model fit, lysimeter specific response to ~~continuous covariates~~ in the fixed part were  
232 included as random slopes. Further, to account for autocorrelative errors according to the time-series origin of the data, a  
233 continuous autocorrelation structure (corCAR1 in *nlme*-package) was defined by the day of the experiment.

234 The drivers of ET: The average air temperature during the course of the experiment was  $17.5^{\circ}\text{C}$  ( $\pm 3.1^{\circ}\text{C}$  – standard  
235 deviation). Among the different plots no systematic variation ~~of~~ temperature, relative humidity and solar radiation was  
236 measured by the microclimate stations ~~underneath the shelters~~.  Summarizing the different atmospheric components defining  
237 rates of ET,  $ET_0$  was calculated. During the duration of experiment the average daily  $ET_0$  was  $3.26 \text{ kgH}_2\text{O m}^{-2} \text{ d}^{-1}$  ( $\pm 1.95$   
238 SD) with a minimum at 0.75 and a maximum of  $6.4 \text{ kgH}_2\text{O m}^{-2} \text{ d}^{-1}$ . However, since  $ET_0$  is subject to short-term natural  
239 variation of the underlying environmental parameters, fluctuations between consecutive days were found to be very  
240 pronounced and no temporal trend was revealed over the period of the experiment (Fig. 2).



241

242 **Fig 2: Atmospheric demand (ET0) and soil water content (SWC) as drivers of ET, A) dynamics of daily average ET0 over the**  
243 **course of the experiment (bold line: all plot average, thin lines: individual plots); B) dynamics of daily average SWC for two**  
244 **vegetation types (S & M, see Table 1) in contrasting irrigation schemes (REG - solid lines, D - dashed lines; bold lines: treatment**  
245 **average; shaded area: standard deviation, thin lines: individual plots); S: Stubai, M: Matsch/Mazia.**

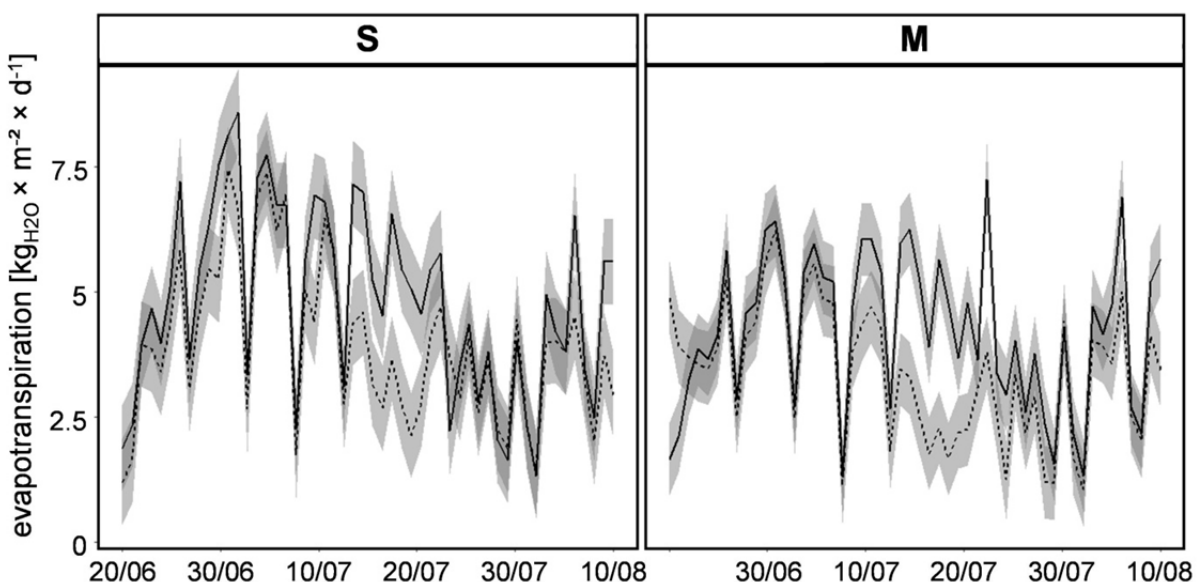
246

247 During the time of the experiment the two contrasting irrigation schemes led to distinct SWC dynamics within the respective  
248 mesocosms (Fig. 2). Since SWC in all lysimeters was high at the beginning of the experiment the value initially decreased in  
249 all plots irrespective of treatment indicating that the water irrigated on plots with regular irrigation did not fully compensate  
250 the loss of water by ET of the corresponding communities. The first clear effects of differential irrigation became only  
251 apparent in the lysimeters with the M-type of vegetation after applying approximately two weeks of drought. Variation in  
252 SWC of lysimeters belonging to the S-type of vegetation was rather strong and it took those units longer to manifest distinct  
253 effects of the different watering schemes. After approximately one month, SWC in both vegetation types revealed clear

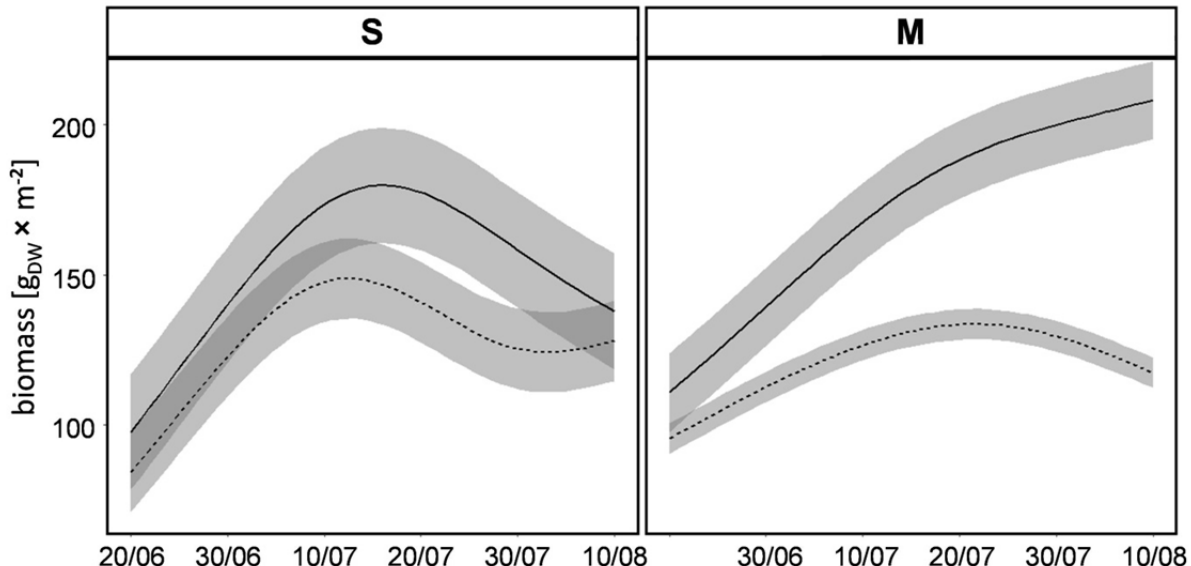




254 effects of the contrasting irrigation strategies. At that time, SWC of both treatments was restored to similar values observed  
255 during the initial stages of the experimental period in order to avoid distress in the drier mesocosms. Rates of daily ET from  
256 the lysimeters were varying very strongly through the period of the experiment and did not reveal a general temporal trend  
257 (Fig. 3). The average evapotranspirative water loss for the lysimeter unit during the duration of the experiment was 4.9   
258 kgH<sub>2</sub>O m<sup>-2</sup> d<sup>-1</sup>. Subject to the atmospheric water vapour pressure deficit the recorded fluxes were characterised by a similar  
259 unsteadiness as the variability of the underlying environmental parameters would suggest. No consistent differences in daily   
260 water flux from the lysimeter mesocosms to the atmosphere could be detected according to the identity of the community.  
261 Also the contrasting irrigation regimes did not impose a overall difference in the rates of ET within the experimental period.   
262 However, during periods of strong divergence of SWC among the two irrigation treatments, daily ET was lower for entities  
263 subjected to experimental drought.



264  
265 Fig 3: Dynamics of daily average ET over the course of the experiment for two different vegetation types (S & M, Table 1)  
266 subjected to contrasting irrigation regimes (REG - solid lines, D - dashed lines; shaded area – standard deviation); S: Stubai, M:  
267 Matsch/Mazia.  
268

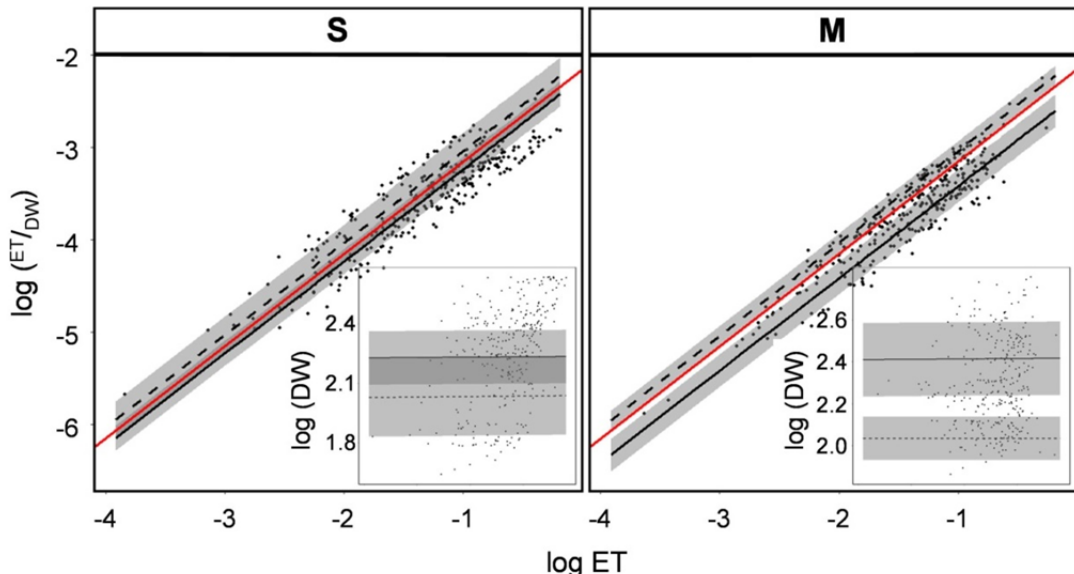


269

270  
271 **Fig 4: Trajectories of biomass development for the two vegetation types (S: Stubai, M: Matsch/Mazia, Table 1) subjected to**  
272 **contrasting irrigation regimes (REG - solid lines, D - dashed lines; shaded area – standard deviation) throughout the duration of**  
273 **the experiment**

274

275 The prediction of biomass development combined from the different non-invasive estimation methods suggested  
276 distinct growth trajectories for the two vegetation types in interaction with the two irrigation regimes. The mesocosms with  
277 communities belonging to the local S-type revealed larger biomass **differentials** during early stages of the experiment  
278 **irrespective of the applied irrigation regime**. However, with increasing duration of the experiment, growth dynamics started  
279 diverging in treatments with contrasting water provision, with biomass differences peaking at the mid-time of the  
280 experimental period. After that peak, the prediction of dry weight suggested a decline in standing biomass for both water  
281 regimes in the S-communities. Towards the end of the experiment, biomasses of communities in the different water  
282 treatments converged to similar values. A different pattern of biomass development was detected for the transplanted  
283 mesocosms (M). From the beginning of the experiment growth processes of the different irrigation treatments yielded  
284 distinct trajectories. In the treatment experiencing regular water provision the biomass gain per unit time was stronger than in  
285 the mesocosms being subjected to irregular watering. That pattern was consistent throughout the experiment, with a strictly  
286 monotonic increase of standing biomass in the M communities of well-watered plots. In contrast, the vegetation of the M-  
287 type in the plots with restricted watering growth started stagnating during the second half of the experimental period. Unlike  
288 the S-type, at the end of the investigation period, biomasses in the M-type communities were clearly distinct according to the  
289 different watering regimes, with the standing mass in the regularly watered plots approximating double the amount  
compared to the treatment with restricted water provision.

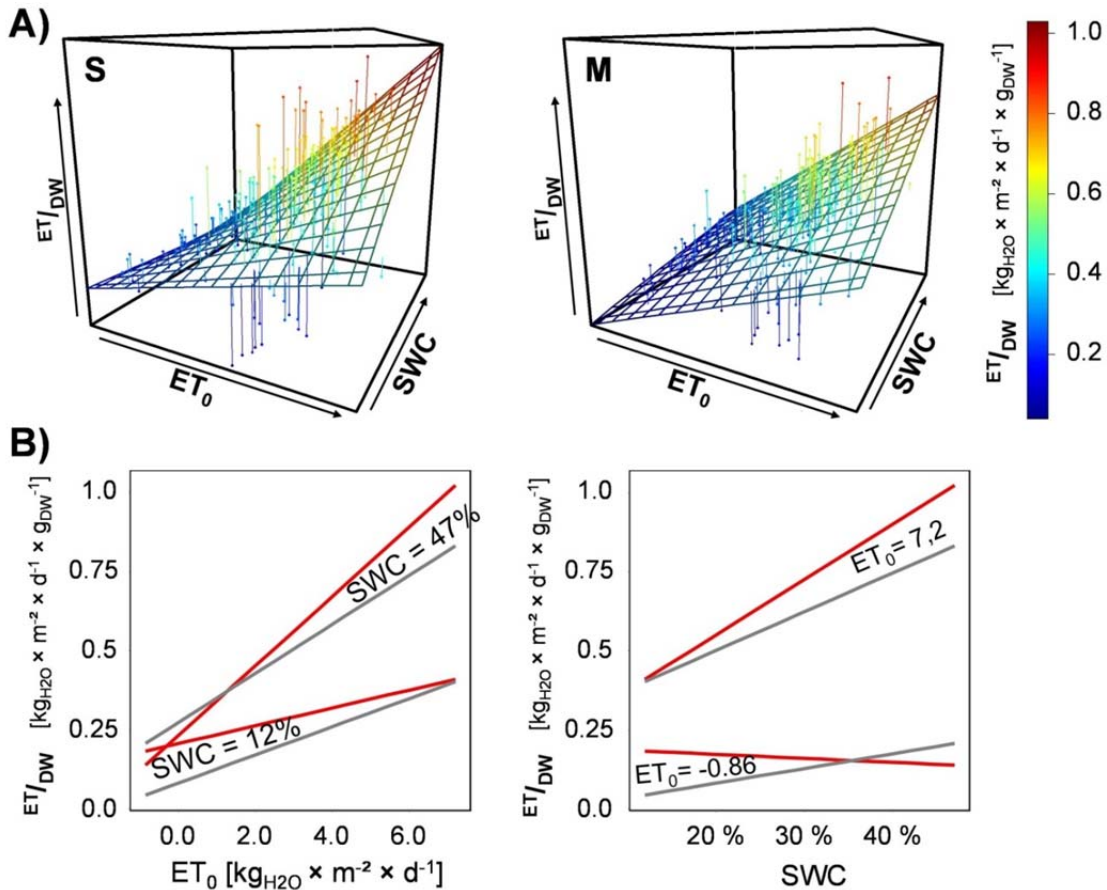


290

291 **Fig 5: Log-log scaling for the two factors defining variability of ET: ET rates per unit dry weight (ET/DW) and standing biomass**  
292 (DW) for the two different vegetation types (S & M, Table 1) subjected to contrasting irrigation regimes (REG - solid  
293 lines, D - dashed lines; shaded area – standard deviation), red line indicates a reference function with the slope of 1.

294

295 Variability of ET is subject to variation in evapotranspiration rates per unit biomass (ET/DW) and the variation in the  
296 standing biomass. Hence, when comparing rates of ET differentiating both underlying components will provide deeper  
297 insights on how the vegetation interface of different communities mediates the water flux from the soil. A strong positive  
298 correlation of total daily ET and ET/DW was found (Fig 5). The log-log-scaling of ET/DW with ET revealed a slope of  
299 0.998 arguing that variation in ET rates measured during the course of this experiment is almost exclusively defined by the  
300 variation in ET rates per unit biomass (100% = 1). This relationship was independent of vegetation type and irrigation  
301 scheme. The effect of biomass variation on the variance of total rates of ET however did have a very small and insignificant  
302 effect. For the local communities (S) the more biomass to be found in the lysimeter mesocosms the bigger was the total daily  
303 water flux to the atmosphere, while the transplanted communities revealed a different pattern. For M-type communities the  
304 amount of biomass in the lysimeters had no strong effect on the rates of total ET. 



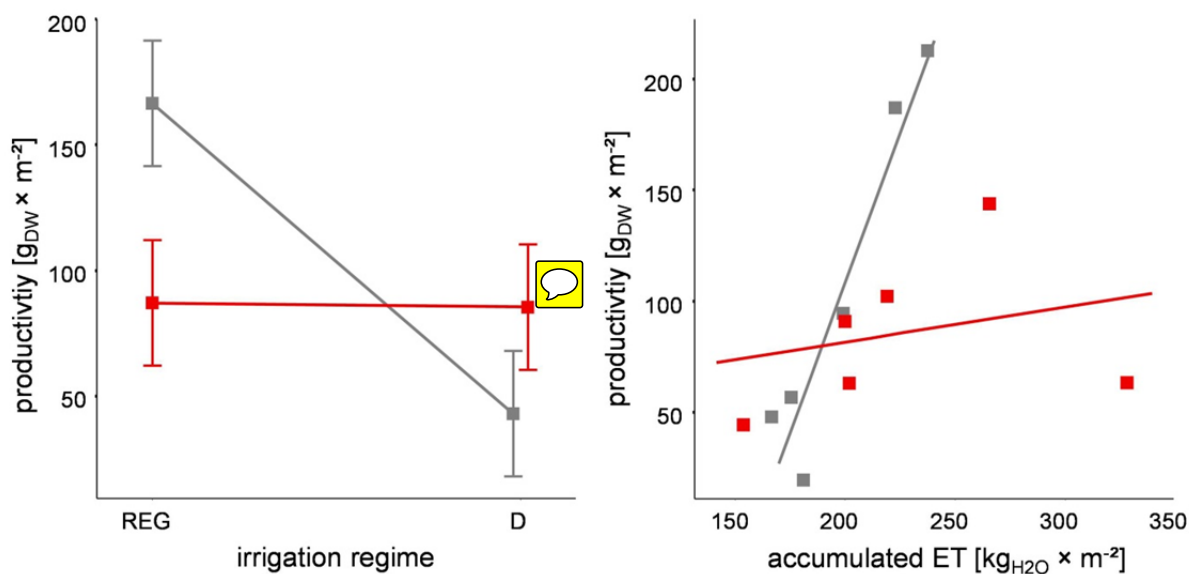
305

306 **Fig 6 A)** 3D plots: response surface of ET per unit DW (ET/DW) along the two-dimensional variation of ET<sub>0</sub> and SWC for the two  
 307 different vegetation types (S: Stubai, M: Matsch/Mazia, Table 1); **B)** projections of ET/DW response along ET<sub>0</sub> and SWC at  
 308 maximum/minimum value of the particular other (red: S-communities, grey: M-communities)

309 After revealing ET/DW as the most important driver in defining variation in the rates of total ET from the lysimeter  
 310 mesocosms, the effect of combined variation in ET<sub>0</sub> and SWC on rates of ET per unit biomass was modelled in dependence  
 311 of the vegetation type (ET/DW = f(ET<sub>0</sub> × SWC × vegetation type)). The average daily sums of ET<sub>0</sub> ranged from -0.75 to a   
 312 maximum of 6.4 kg<sub>H2O</sub> m<sup>-2</sup> d<sup>-1</sup>, while the averaged SWC realized during the duration of the experiment covered a range from  
 313 approximately 12-47% (Fig. 5). Both, ET<sub>0</sub> and SWC had a highly significant and positive effect on achieved rates of ET/DW  
 314 (Fig. 6, **Table 2**). However, as implied by a significant synergistic interaction of ET<sub>0</sub> and SWC, rates of ET/DW increased  
 315 stronger if SWC and ET<sub>0</sub> increased concurrently than the individual gradients of either would imply (Fig 6.). With increasing  
 316 ET<sub>0</sub> the response of ET/DW was stronger the higher SWC was. However, there was a significant difference how both  
 317 vegetation types responded within the landscape of environmental drivers defining ET/DW (Table 2). The local (S)  
 318 vegetation had higher rates of ET/DW - when both ET<sub>0</sub> and SWC were low - than the transplanted vegetation type (M),  
 319 suggesting a higher base rate of ET/DW. On the low end of investigated SWC the M-vegetation had a stronger response to



320 ET<sub>0</sub> than the local S-vegetation. Despite that stronger response of the transplanted vegetation (M) along the ET<sub>0</sub> gradient at  
 321 low SWC, the maximum rates of ET/DW converted to similar values due to the higher base flux at low ET<sub>0</sub>/ low SWC in the  
 322 S-vegetation. In turn, under conditions of high soil water availability the ET<sub>0</sub>-response of the S-type was much more  
 323 pronounced than in the M-type. A similar pattern was found comparing the SWC-response of both vegetation types for the  
 324 range of different ET<sub>0</sub> values realized during the experiment. At low ET<sub>0</sub> the M-type vegetation responded stronger to  
 325 variations in SWC, while there was almost no response in the S-type. However, at high ET<sub>0</sub> the response of the S-type to  
 326 increasing SWC was again much more pronounced than in lysimeters with the M-type. Because of the higher rates of  
 327 ET/DW at low ET<sub>0</sub>/SWC and the overall increased response potential of the S-type vegetation, the ET/DW values achieved  
 328 in the M-communities stayed below those found in the local vegetation for almost the entire range of combinations between  
 329 ET<sub>0</sub> and SWC investigated in this experiment.



330  
 331 **Fig 7: Productivity of two vegetation types (± standard error, Stubai - red & Matsch/Mazia - grey; Table 1) subjected to**  
 332 **contrasting irrigation schemes (Fig 1), right panel: dry matter productivity of two vegetation types (see above) as function of**  
 333 **accumulated evapotranspiration over the experimental duration**

334 Comparing the productivity of the two vegetation types among the two irrigation treatments revealed a contrasting  
 335 response for the DW productivity (Fig. 7, left panel). For the local S-Type the biomass gain over the experimental period did  
 336 not show a strong dependence on the applied watering regime. The productivity of the S-type stayed well below from what  
 337 would be expected for the vegetation outside the experimental site in both treatments. For the M-communities, however,  
 338 productivity was on average more than two fold higher in the plots experiencing regular water provision compared to those  
 339 exposed to extended periods of drought.

340 Integrated over the entire experimental period, the biomass productivity per unit water was significantly higher for the  
 341 transplanted mesocosms M (Fig 7, right panel). The data suggested a productivity increase of 2.6 g<sub>DW</sub> per kg of water for the



342 M vegetation. In contrast, for the S-type mesocosms the average increase of productivity per 1kg of evapotranspiration was  
343 approximately only 0.16g. This pattern suggests that biomass generation in the M-type vegetation is significantly more  
344 dependent on water availability, while the differences in the slope imply lower efficiency of water use with respect to dry  
345 weight accumulation in the S mesocosms.



346

347 It is intuitive to understand, that  $ET_0$  and SWC impose independent and interacting effects on water fluxes from the  
348 soil to the atmosphere with one of either constraining the total rates of ecosystem ET (Kim and Verma, 1991; Perez et al.,  
349 2006). Beyond the effects of these abiotic drivers, the measurements of the present experiment reveal a community specific  
350 signal in the definition of ecosystem water exchange. The community specific configuration of the soil-plant-atmosphere  
351 interface is instinctively acknowledged if distinct vegetation types are compared. Water fluxes from the system will to some  
352 degree always scale with productivity and total biomass of the vegetation (Zeppel et al., 2014 and references therein). This  
353 context will drive variation in ET of contrasting biomes together with environmental parameters affecting the availability of  
354 water and the atmospheric deficit.

355 However, results of this experiment reveal that vegetation specific differences have a component, which defines  
356 ecosystem water flux beyond the impact of variations in total biomass. Such differences will be important to understand and  
357 to consider if communities of the same type need to be evaluated with respect to their particular impact on the hydrological  
358 regulation of the ecosystem. The response of water fluxes along co-operating gradients of SWC and  $ET_0$  indicated  
359 divergence in the conductance potential of the two alpine grassland communities, which were independent from the biomass  
360 present. At low SWC the response of the M-type to increasing  $ET_0$  was much stronger than for the S-type arguing for a  
361 higher efficiency to mobilise limited water resources from the soil column. Conversely, under conditions of high soil water  
362 availability water fluxes from the S-type responded much stronger to increases of  $ET_0$  suggesting a higher overall  
363 conductance potential. Similar implications were revealed along the gradient of soil water availability. SWC variations had  
364 almost no effect on the S-type communities when the atmospheric draw was small, while the M-type mesocosm still  
365 mediated fluxes to the atmosphere. Under high  $ET_0$  however, the divergence in the response of ET between S & M-  
366 communities to varying SWC suggests that, from starting at similar rates, the S-type became much more efficient to conduct  
367 water to the atmosphere the less soil water became limiting. These differences between the two vegetation types indicate  
368 different strategies in the water utilisation. For the M-type this strategy may be summarized by a high potential to utilize  
369 even scarce water resources, a lower potential to translate atmospheric deficits into higher water conductance with rates of  
370 ET staying below those measured for the S-type for most environmental scenarios included within the experimental period.  
371 This implies an overall conservative and water saving strategy. For the S-communities, in contrast, which show high water  
372 conductance potential with strongly increasing ET rates when environmental conditions become less constraining, an  
373 acquisitive strategy is suggested. With high rates even at base level these communities appear not to be optimized to save



374 water and might experience drought effects earlier and probably stronger, when water availability becomes limiting. There  
375 might be some dampening effect as soil hydrological properties indicate a higher amount of plant available water for the S-  
376 type. The permanent wilting point (pF 4.2) in the main rooting zone (averaged values for 0.05m, 0.15m, 0.25m soil depth)  
377 was at a SWC of 13% ( $\pm$  8.3 SD) and 17% ( $\pm$  3.1 SD) for the S-vegetation type and the M-vegetation type, respectively.  
378 Whereas field capacity (pF 2.1) was found to be at a SWC of 46% ( $\pm$  4.4 SD) and 43% ( $\pm$  6.8%) for the S-vegetation type  
379 and the M-vegetation type, respectively. In summary, the plant available water was found to be 33 vol% for the S-type and  
380 26 vol% for the M-type. However, the variation at 0.05m soil depth was very low and even a slightly higher amount of plant  
381 available water was found for the M-type (S-type: 28 vol%; M-type: 29 vol%) at this soil depth. Although soil hydrological  
382 properties play a role in the community specific conductance potential of soil water to the atmosphere, differences found for  
383 the investigated two different vegetation types turned out to be not decisive in this context.

384 Sharing a common environment, the differences in biomass-independent conductance potential between the two  
385 Alpine grassland communities are likely to have a foundation in a contrasting physiological, functional and structural  
386 organisation of the vegetation. Functional divergence in water utilisation, evapotranspiration and other aspects of  
387 hydrological regulation of ecosystems (e.g. infiltration, surface run-off) between communities can be manifested by the  
388 frequency distribution in the values of particular traits (Díaz et al., 2013). Canopy complexity - density and size, growth  
389 form composition, composition and diversity of vascular structures, stomatal density and conductance mediate community  
390 specific differences in the evapotranspiration aboveground (de Bello et al., 2010) Belowground, the structure and depth of  
391 the individual rooting systems is an important determinant for the water utilisation potential of communities (Knapp et al.,  
392 2008). Along the variation and composition of these traits water usage and consequently also drought resistance of  
393 contrasting communities is defined. The differences in the two vegetation types suggest high exploitation potential for scarce  
394 soil water, probably facilitated by a higher priority on water exploitation in the soil in the M-mesocosms and, conversely, a  
395 stronger importance on aboveground structures mediating light capture and gas-exchange, leading to an increased response  
396 potential of ET for atmospheric triggers in the local S-communities.

397 The clear vegetation response to variable water availability observed in the present experiment is not common in  
398 studies targeting Alpine grasslands (de Bello et al., 2010). Based on multi-annual measurements of evapotranspiration at 16  
399 sites in the Austrian Alps, it was suggested, that even during years with low annual precipitation Alpine grasslands do not  
400 experience water stress (Wieser et al., 2008). Gilgen and Buchmann (2009) could not conclude on a general drought  
401 response of grasslands in Switzerland, while acknowledging a site-specific impact with communities receiving less annual  
402 precipitation being more susceptible to drought stress than those at higher rainfall levels. Also arguing for a co-defined and  
403 interactive manifestation in the effects of varying water availability, a strong drought response of Alpine grassland  
404 functioning was revealed under scenarios of co-occurring heat waves (De Boeck et al., 2016). A modelling study for  
405 grassland ecosystems in the Austrian- and French Alps suggested a higher vulnerability to drought for communities with a  
406 water spending strategy targeting on water provision of the ecosystems in general (Leitinger et al., 2015). However, it seems  
407 inappropriate to synthesize a general summary on the response of Alpine grasslands to variations in water availability given



408 the small body of research performed. Considering the different spatio-temporal scales, the range of parameters measured,  
409 and the management and biodiversity spectrum of different grassland types in the Alps, drawing broad and universal  
410 generalisation yet becomes unrewarding. For experiments with contrasting treatments the practicalities of manipulating  
411 water availability potentially also need to be considered for the interpretation of the results.

412 Drought scenarios are usually generated by rain-out shelters using a UV-permeable, transparent film for roofing. If  
413 compared to unroofed controls, temperature differences and attenuation of photosynthetically active radiation reducing total  
414 productivity will have to be expected as pure artefacts of the sheltering (Vogel et al., 2013). However, even if both  
415 treatments are sheltered, differential irrigation may not immediately lead to the realisation of varying water availabilities.  
416 The beginning of the present experiment was marked by the establishment of the rain-out shelters and the omission of  
417 irrigation in the treatments with irregular watering (D). From this point, it took approximately two weeks for the SWC of  
418 both irrigation schemes to diverge significantly in M-type mesocosms, for the S-type even longer. Therefore, regular  
419 irrigation and, respectively, its omission can, counter-intuitively, only be an indicator of contrasting water availability. The  
420 establishment of drought conditions in the strict sense of a depleted soil water reservoir is realized by the interaction of pre-  
421 treatment SWC, standing biomass and atmospheric effects. Variations in vegetation water status have to be defined in  
422 context of water availability (supply) and physiology, phenology and the leaf-to-air evaporative gradient (Gilbert and  
423 Medina, 2016). The beginning of the experiment was characterized by combination of days with consistently high averages  
424 of  $ET_0$  and high SWC in all mesocosms. This combination led to high ET and a decrease of SWC for all experimental units.  
425 Due to the parallel decline of SWC irrespective the watering regime applied, the water availability differentiation among the  
426 treatments was delayed. For such reasons, it was argued to define variations in water availability not purely on the basis of  
427 contrasting regimes of water input (i.e. irrigated vs. non-irrigated) if these are not causing systematic variations in soil  
428 moisture (Kramer, 1983). Defining water supply based on the continuous range of SWC rather than discrete irrigation  
429 treatments considers soil type specific characteristics of matric potential and hydraulic conductivity. Also practical problems  
430 with realizing discrete treatments of water availability in the field (i.e. precipitation entry to sheltered plots due to heavy  
431 winds, spatio-temporal variation in the effectiveness of automated irrigation) will be migrated by referencing ecosystem  
432 responses to gradients of water supply. Defining vegetation responses along continuous ranges of environmental factors will  
433 further yield stronger information about the response surface of the system and improves model building and testing (Beier  
434 et al., 2012).

435 Irrespective the variability of different water availabilities within the two irrigation regimes, mesocosms subjected to  
436 regular watering (REG) had on average a higher productivity than those with irregular and in total less irrigation. However,  
437 significant differences between the different communities were found in the response to variations in the water supply (Fig  
438 7). Relating total productivity to the amount of evapotranspirative water release over the experimental period revealed a  
439 higher biomass gain per unit water in the M-type communities. The higher water use efficiency in the biomass production of  
440 these mesocosms together with their overall stronger water saving strategy reinforces their optimisation to scarce water  
441 supply. For the local S-communities, in contrast, the low biomass differential per unit water consumption indicates a high



442 potential to conduct water from the soil to the atmosphere and that productivity of this vegetation is probably not often  
443 constrained by water availability in its natural context. (Brilli et al., 2011) expect from a water spending strategy to have a  
444 cooling feedback in terms of climate warming. However, a negative feedback for water provision services (i.e. down-stream  
445 water users) has to be expected. Further decisive changes remain debatable: How will 'water spending' plant communities  
446 adapt if droughts occur more frequently and possibly with higher intensities (Bahn et al., 2014; Reichstein et al., 2013). To  
447 what extent play – at least initially - physiological and morphological changes a role or is there an immediate shift to a better  
448 adapted community?

449

450 We wish to thank Valentin Schießendoppler, Jana Schönherr and Jakob Fitzner for their help in the field and during  
451 the analysis in the lab. The funding partners that have supported this research include the project ClimAgro (Autonome  
452 Provinz Bozen – Südtirol, Abteilung Bildungsförderung, Universität und Forschung) and the Austrian Federal Ministry of  
453 Science, Research and Economy with the HRSM – cooperation project KLIMAGRO. This study was conducted on the  
454 LTER site 'Stubai Valley' (LTSEER platform 'Tyrolean Alps') and the LTSEER platform 'Val Mazia/Matschertal'). Both sites  
455 belong to the national and international Long-Term Ecological Research Networks (LTER-Austria, LTER-Italy, LTER-  
456 Europe and ILTER). UT and GL are part of the research focus 'Alpine Space – Man and Environment' at the University of  
457 Innsbruck.

458

## 459 References

460 Allen, R. G., Pereira, L. S., Raes, D., and Smith, M.: Crop evapotranspiration - Guidelines for computing crop water  
461 requirements - FAO Irrigation and drainage paper 56, FAO, Rome, Italy, 1998.

462 Auer, I., Böhm, R., Jurkovic, A., Lipa, W., Orlik, A., Potzmann, R., Schöner, W., Ungersböck, M., Matulla, C., Briffa, K.,  
463 Jones, P., Efthymiadis, D., Brunetti, M., Nanni, T., Maugeri, M., Mercalli, L., Mestre, O., Moisselin, J.-M., Begert,  
464 M., Müller-Westermeier, G., Kveton, V., Bochnicek, O., Stastny, P., Lapin, M., Szalai, S., Szentimrey, T., Cegnar, T.,  
465 Dolinar, M., Gajic-Capka, M., Zaninovic, K., Majstorovic, Z., and Nieplova, E.: HISTALP—historical instrumental  
466 climatological surface time series of the Greater Alpine Region, International Journal of Climatology, 27, 17-46,  
467 2007.

468 Bahn, M., Reichstein, M., Dukes, J. S., Smith, M. D., and McDowell, N. G.: Climate–biosphere interactions in a more  
469 extreme world, New Phytologist, 202, 356-359, 2014.



470 Beier, C., Beierkuhnlein, C., Wohlgemuth, T., Penuelas, J., Emmett, B., Körner, C., de Boeck, H., Christensen, J. H.,  
471 Leuzinger, S., Janssens, I. A., and Hansen, K.: Precipitation manipulation experiments – challenges and  
472 recommendations for the future, *Ecology Letters*, 15, 899-911, 2012.

473 Beniston, M.: Impacts of climatic change on water and associated economic activities in the Swiss Alps, *Journal of*  
474 *Hydrology*, 412, 291-296, 2012.

475 Beniston, M.: Mountain Climates and Climatic Change: An Overview of Processes Focusing on the European Alps, *pure and*  
476 *applied geophysics*, 162, 1587-1606, 2005.

477 Beniston, M., Stephenson, D. B., Christensen, O. B., Ferro, C. A. T., Frei, C., Goyette, S., Halsnaes, K., Holt, T., Jylhä, K.,  
478 Koffi, B., Palutikof, J., Schöll, R., Semmler, T., and Woth, K.: Future extreme events in European climate: an  
479 exploration of regional climate model projections, *Climatic Change*, 81, 71-95, 2007.

480 Bogaña, H., Schulz, K., and Vereecken, H.: Towards a network of observatories in terrestrial environmental research, *Adv.*  
481 *Geosci.*, 9, 109-114, 2006.

482 Böhm, R., Auer, I., Brunetti, M., Maugeri, M., Nanni, T., and Schöner, W.: Regional temperature variability in the European  
483 Alps: 1760–1998 from homogenized instrumental time series, *International Journal of Climatology*, 21, 1779-1801,  
484 2001.

485 Brilli, F., Hörtnagl, L., Hammerle, A., Haslwanter, A., Hansel, A., Loreto, F., and Wohlfahrt, G.: Leaf and ecosystem  
486 response to soil water availability in mountain grasslands, *Agricultural and Forest Meteorology*, 151, 1731-1740,  
487 2011.

488 Ciccarelli, N., von Hardenberg, J., Provenzale, A., Ronchi, C., Vargiu, A., and Pelosini, R.: Climate variability in north-  
489 western Italy during the second half of the 20th century, *Global and Planetary Change*, 63, 185-195, 2008.

490 de Bello, F., Lavorel, S., Díaz, S., Harrington, R., Cornelissen, J. H. C., Bardgett, R. D., Berg, M. P., Cipriotti, P., Feld, C.  
491 K., Hering, D., Martins da Silva, P., Potts, S. G., Sandin, L., Sousa, J. P., Storkey, J., Wardle, D. A., and Harrison, P.  
492 A.: Towards an assessment of multiple ecosystem processes and services via functional traits, *Biodiversity and*  
493 *Conservation*, 19, 2873-2893, 2010.

494 De Boeck, H. J., Bassin, S., Verlinden, M., Zeiter, M., and Hiltbrunner, E.: Simulated heat waves affected alpine grassland  
495 only in combination with drought, *New Phytologist*, 209, 531-541, 2016.



496 Díaz, S., Purvis, A., Cornelissen, J. H. C., Mace, G. M., Donoghue, M. J., Ewers, R. M., Jordano, P., and Pearse, W. D.:  
497 Functional traits, the phylogeny of function, and ecosystem service vulnerability, *Ecology and Evolution*, 3, 2958-  
498 2975, 2013.

499 Estiarte, M., Vicca, S., Peñuelas, J., Bahn, M., Beier, C., Emmett, B. A., Fay, P. A., Hanson, P. J., Hasibeder, R., Kigel, J.,  
500 Kröel-Dulay, G., Larsen, K. S., Lellei-Kovács, E., Limousin, J.-M., Ogaya, R., Ourcival, J.-M., Reinsch, S., Sala, O.  
501 E., Schmidt, I. K., Sternberg, M., Tielbörger, K., Tietema, A., and Janssens, I. A.: Few multiyear precipitation-  
502 reduction experiments find a shift in the productivity-precipitation relationship, *Global Change Biology*, 22, 2570-  
503 2581, 2016.

504 Gilbert, M. E. and Medina, V.: Drought Adaptation Mechanisms Should Guide Experimental Design, *Trends in Plant  
505 Science*, 21, 639-647, 2016.

506 Gilgen, A. K. and Buchmann, N.: Response of temperate grasslands at different altitudes to simulated summer drought  
507 differed but scaled with annual precipitation, *Biogeosciences*, 6, 2525-2539, 2009.

508 Gobiet, A., Kotlarski, S., Beniston, M., Heinrich, G., Rajczak, J., and Stoffel, M.: 21st century climate change in the  
509 European Alps—A review, *Science of The Total Environment*, 493, 1138-1151, 2014.

510 Heimann, M. and Reichstein, M.: Terrestrial ecosystem carbon dynamics and climate feedbacks, *Nature*, 451, 289-292,  
511 2008.

512 IPCC: Climate Change 2013: The Physical Science Basis. Contribution of Working Group I to the Fifth Assessment Report  
513 of the Intergovernmental Panel on Climate Change, Cambridge, United Kingdom and New York, NY, USA, 1535  
514 pp., 2013.

515 IPCC: Managing the Risks of Extreme Events and Disasters to Advance Climate Change Adaptation. A Special Report of  
516 Working Groups I and II of the Intergovernmental Panel on Climate Change, Cambridge University Press,  
517 Cambridge, UK and New York, NY, USA, 2012.

518 Jasechko, S., Sharp, Z. D., Gibson, J. J., Birks, S. J., Yi, Y., and Fawcett, P. J.: Terrestrial water fluxes dominated by  
519 transpiration, *Nature*, 496, 347-350, 2013.

520 Jonasson, S.: Evaluation of the Point Intercept Method for the Estimation of Plant Biomass, *Oikos*, 52, 101-106, 1988.

521 Kim, J. and Verma, S. B.: Modeling canopy stomatal conductance in a temperate grassland ecosystem, *Agricultural and  
522 Forest Meteorology*, 55, 149-166, 1991.



523 Knapp, A. K., Beier, C., Briske, D. D., Classen, A. T., Luo, Y., Reichstein, M., Smith, M. D., Smith, S. D., Bell, J. E., Fay,  
524 P. A., Heisler, J. L., Leavitt, S. W., Sherry, R., Smith, B., and Weng, E.: Consequences of More Extreme Precipitation  
525 Regimes for Terrestrial Ecosystems, *BioScience*, 58, 811-821, 2008.

526 Kramer, P. J.: *Water Relations of Plants*, Academic Press, 1983.

527 Lati, R. N., Manevich, A., and Filin, S.: Three-dimensional image-based modelling of linear features for plant biomass  
528 estimation, *International Journal of Remote Sensing*, 34, 6135-6151, 2013.

529 Leitinger, G., Ruggenthaler, R., Hammerle, A., Lavorel, S., Schirpke, U., Clement, J.-C., Lamarque, P., Obojes, N., and  
530 Tappeiner, U.: Impact of droughts on water provision in managed alpine grasslands in two climatically different  
531 regions of the Alps, *Ecohydrology*, 8, 1600-1613, 2015.

532 Machado, S., Bynum, E. D., Archer, T. L., Lascano, R. J., Wilson, L. T., Bordovsky, J., Segarra, E., Bronson, K., Nesmith,  
533 D. M., and Xu, W.: Spatial and Temporal Variability of Corn Growth and Grain Yield This research was supported  
534 by the Texas State Legislature Initiative on Precision Agriculture for the Texas High Plains, *Crop Science*, 42, 1564-  
535 1576, 2002.

536 Messerli, B., Viviroli, D., and Weingartner, R.: Mountains of the world: Vulnerable Water Towers for the 21(st) century,  
537 *Ambio*, 2004. 29-34, 2004.

538 Newesely, C., Leitinger, G., Zimmerhofer, W., Kohl, B., Markart, G., Tasser, E., and Tappeiner, U.: Rain simulation in  
539 patchy landscapes: Insights from a case study in the Central Alps, *CATENA*, 127, 1-8, 2015.

540 Peñuelas, J., Gordon, C., Llorens, L., Nielsen, T., Tietema, A., Beier, C., Bruna, P., Emmett, B., Estiarte, M., and Gorissen,  
541 A.: Nonintrusive Field Experiments Show Different Plant Responses to Warming and Drought Among Sites, Seasons,  
542 and Species in a North–South European Gradient, *Ecosystems*, 7, 598-612, 2004.

543 Perez, P. J., Lecina, S., Castellvi, F., Martínez-Cob, A., and Villalobos, F. J.: A simple parameterization of bulk canopy  
544 resistance from climatic variables for estimating hourly evapotranspiration, *Hydrological Processes*, 20, 515-532,  
545 2006.

546 Peters, A., Nehls, T., Schonsky, H., and Wessolek, G.: Separating precipitation and evapotranspiration from noise &ndash; a  
547 new filter routine for high-resolution lysimeter data, *Hydrol. Earth Syst. Sci.*, 18, 1189-1198, 2014.

548 R Development Core Team: R: A language and environment for statistical computing. R Foundation for Statistical  
549 Computing, Vienna, Austria, 2015.



550 551 Rebetez, M. and Reinhard, M.: Monthly air temperature trends in Switzerland 1901–2000 and 1975–2004, Theoretical and  
Applied Climatology, 91, 27-34, 2008.

552 553 554 Reichstein, M., Bahn, M., Ciais, P., Frank, D., Mahecha, M. D., Seneviratne, S. I., Zscheischler, J., Beer, C., Buchmann, N.,  
Frank, D. C., Papale, D., Rammig, A., Smith, P., Thonicke, K., van der Velde, M., Vicca, S., Walz, A., and  
Wattenbach, M.: Climate extremes and the carbon cycle, Nature, 500, 287-295, 2013.

555 556 557 Renton, M. and Poorter, H.: Using log–log scaling slope analysis for determining the contributions to variability in  
biological variables such as leaf mass per area: why it works, when it works and how it can be extended, New  
Phytologist, 190, 5-8, 2011.

558 559 Schindler, U.: A rapid method for measuring the hydraulic conductivity in cylinder core samples from unsaturated soil,  
Archiv fur Acker- und Pflanzenbau und Bodenkunde, 24, 1-7, 1980.

560 561 562 Schrader, F., Durner, W., Fank, J., Gebler, S., Pütz, T., Hannes, M., and Wollschläger, U.: Estimating Precipitation and  
Actual Evapotranspiration from Precision Lysimeter Measurements, Procedia Environmental Sciences, 19, 543-552,  
2013.

563 564 Silva, L. C. R.: From air to land: understanding water resources through plant-based multidisciplinary research, Trends in  
Plant Science, 20, 399-401, 2015.

565 566 Solomon, S., Plattner, G.-K., Knutti, R., and Friedlingstein, P.: Irreversible climate change due to carbon dioxide emissions,  
Proceedings of the National Academy of Sciences, 106, 1704-1709, 2009.

567 568 569 570 Tackenberg, O.: A New Method for Non-destructive Measurement of Biomass, Growth Rates, Vertical Biomass Distribution  
and Dry Matter Content Based on Digital Image AnalysisTackenberg — Image Analysis for Non-destructive Biomass  
MeasurementTackenberg — Image Analysis for Non-destructive Biomass Measurement, Annals of Botany, 99, 777-  
783, 2007.

571 572 van der Schrier, G., Efthymiadis, D., Briffa, K. R., and Jones, P. D.: European Alpine moisture variability for 1800–2003,  
International Journal of Climatology, 27, 415-427, 2007.

573 574 Vivioli, D., Weingartner, R., and Messerli, B.: Assessing the Hydrological Significance of the World's Mountains,  
Mountain Research and Development, 23, 32-40, 2003.



575 Vogel, A., Fester, T., Eisenhauer, N., Scherer-Lorenzen, M., Schmid, B., Weisser, W. W., and Weigelt, A.: Separating  
576 Drought Effects from Roof Artifacts on Ecosystem Processes in a Grassland Drought Experiment, PLOS ONE, 8,  
577 e70997, 2013.

578 Wieser, G., Hammerle, A., and Wohlfahrt, G.: The Water Balance of Grassland Ecosystems in the Austrian Alps, Arctic,  
579 Antarctic, and Alpine Research, 40, 439-445, 2008.

580 Wohlfahrt, G., Hammerle, A., Haslwanter, A., Bahn, M., Tappeiner, U., and Cernusca, A.: Seasonal and inter-annual  
581 variability of the net ecosystem CO<sub>2</sub> exchange of a temperate mountain grassland: Effects of weather and  
582 management, Journal of Geophysical Research: Atmospheres, 113, n/a-n/a, 2008.

583 Zacharias, S., Bogena, H., Samaniego, L., Mauder, M., Fuß, R., Pütz, T., Frenzel, M., Schwank, M., Baessler, C.,  
584 Butterbach-Bahl, K., Bens, O., Borg, E., Brauer, A., Dietrich, P., Hajnsek, I., Helle, G., Kiese, R., Kunstmann, H.,  
585 Klotz, S., Munch, J. C., Papen, H., Priesack, E., Schmid, H. P., Steinbrecher, R., Rosenbaum, U., Teutsch, G., and  
586 Vereecken, H.: A Network of Terrestrial Environmental Observatories in Germany, Vadose Zone Journal, 10, 955-  
587 973, 2011.

588 Zeppel, M. J. B., Wilks, J. V., and Lewis, J. D.: Impacts of extreme precipitation and seasonal changes in precipitation on  
589 plants, Biogeosciences, 11, 3083-3093, 2014.